

Issues Regarding Acceleration in Crystals*

PISIN CHEN

*Stanford Linear Accelerator Center
Stanford University, Stanford, California 94309*

DAVID B. CLINE AND WILLIAM E. GABELLA

*Department of Physics,
University of California, Los Angeles, CA 90024*

ABSTRACT

Both self-acceleration and laser-acoustic acceleration in crystals are considered. The conduction electrons in the crystal are treated as a plasma and are the medium through which the acceleration takes place. Self-acceleration is the possible acceleration of part of a bunch due to plasma oscillations driven by the leading part. Laser-acoustic acceleration uses a laser in quasi-resonance with an acoustic wave to pump up the plasma oscillation to accelerate a beam. Self-driven schemes though experimentally simple seem problematic because single bunch densities must be large.

INTRODUCTION

For making dramatically higher gradients in future generations of high energy particle accelerators and for making low energy accelerators more accessible, it would be useful to have a solid state accelerator^[1,2] capable of sustaining very high accelerating gradients. The conduction electrons in the solid already make a convenient source of plasma, hence one can invoke all the concepts concerning plasma acceleration and focusing.^[3] Also channeling in crystalline solids, the confinement of positively charged particles between planes of atoms (planar channeling), leads to transverse confinement of the beam and preservation of the beam size. These properties encourage the investigation of using crystalline solids as accelerators.

Solid state accelerators were discussed previously by Chen and Noble^[1] especially from the point of view of emittance preservation and possible external mechanisms for driving the plasma oscillation. They take as their model that the crystal is just a bag of plasma and it is the plasma interactions, appropriately modified by the crystal structure, that determine focusing and acceleration of a traversing charged particle beam.

* Work supported by the Department of Energy, contract DE-AC03-76SF00515.

One reason for the excitement over both plasma and solid state acceleration is that in the cold wave-breaking limit of the plasma-fluid equations, the largest electric fields that can occur are the order of $\sqrt{n_0}$ V/cm when the plasma density n_0 is given in particles per cm^3 . So for a metal with conduction electron density around $10^{22}/\text{cm}^3$, one might expect 100 GeV/cm accelerating gradient. Though practical concerns and instabilities will yield an actual gradient far below this limit.

There are issues that arise about how the crystal structure modifies the physical properties of the free conduction band electrons in the solid when it performs plasma oscillations. One is whether the effective mass or the usual mass of the electron is relevant. For this paper, the plasma oscillations do not carry out such bulk motion that the lattice will modify the behavior of the electron significantly. So, currently it seems appropriate to use the free space rest mass of the electron for the remainder of this paper.

In the following, the self-focusing and self-acceleration of a relativistic beam in a plasma are reviewed, the laser-acoustic accelerator is discussed, and issues concerning radiation in solids are briefly mentioned. Finally, some conclusions as to the best possible approach for testing the ideas of solid-state acceleration are given.

BEAM SELF-ACCELERATION

As a bunched beam enters a plasma, whether the source of that plasma is a solid or not, it very quickly sets up plasma oscillations which in turn can act back on the beam. The principle of self-focusing of a relativistic beam in a plasma is one such consequence.^[4] For the discussion presented here, the plasma begins with an unperturbed plasma density of n_0 .

In Ref. 4 the focusing fields for a parabolic shaped bunch are calculated. Since this is done in the language of wake fields, it is quite straight forward to use the Panofsky-Wenzel theorem (or Greens theorem) to find the longitudinal fields. The bunch distribution that generates the wake fields is parabolic,

$$\sigma(x) = \rho_b \left(1 - \frac{r^2}{a^2}\right) \left(1 - \frac{(\zeta + b)^2}{b^2}\right) , \quad (1)$$

with $\rho_b = 3N/(2\pi a^2 b)$ where N is the bunch population. The longitudinal coordinate ζ is the usual co-moving coordinate $z - ct$; the head of the bunch is at $\zeta = 0$ and the tail is at $\zeta = -2b$. Using this distribution and the linearized cold fluid equations for a plasma perturbation, the cylindrically symmetric wake fields are

$$eW_{\perp} = \frac{8\pi e^2 \rho_b}{k} \left[I_1(kr) K_2(ka) - \frac{r}{ka^2} \right] \times \\ \left[\left(1 - \frac{(\zeta + b)^2}{b^2}\right) + \frac{2}{kb} \sin k\zeta + \frac{2}{k^2 b^2} (1 - \cos k\zeta) \right] , \quad (2)$$

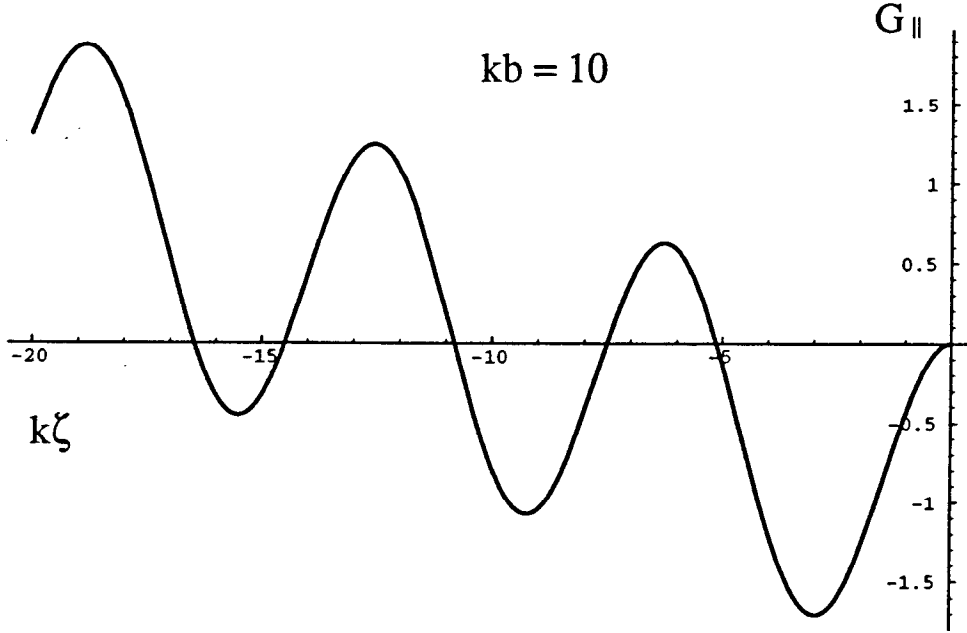


Figure 1. The longitudinal dependence of the longitudinal wake field for $kb = 10$. The middle of the bunch is at $k\zeta = -10$.

for the transverse field on a test particle, and

$$eW_{\parallel} = \frac{16\pi e^2 \rho_b}{k^2 b} \left[I_0(kr)K_2(ka) + \frac{1}{2}(1 - r^2/a^2) - \frac{2}{k^2 a^2} \right] \times \left[\cos k\zeta - \left(\frac{\zeta + b}{b} \right) + \frac{1}{kb} \sin k\zeta \right] , \quad (3)$$

for the longitudinal field on a test particle. The wave number for the plasma oscillation has been used and is $k^2 = \omega^2/c^2 = 4\pi n_0 r_e$, where r_e is the classical electron radius.

For ease of notation and since we are usually considering either the longitudinal or the transverse dependence of the wake fields, the following notation is introduced: $eW_{\perp} = 16\pi e^2 \rho_b F_{\perp}(r)G_{\perp}(\zeta)/k$ and $eW_{\parallel} = 16\pi e^2 \rho_b F_{\parallel}(r)G_{\parallel}(\zeta)/k^2 b$. So, the F_{\perp} and the F_{\parallel} are the expressions in the first set of [...] in (2) and (3), and the G 's are the terms in the second set of brackets with the left over coefficients.

In Figure 1, G_{\parallel} is plotted for $kb = 10$ and as a function of the dimensionless parameter $k\zeta$. Notice the rising trend toward the bunch tail ($\zeta = -2b$), this is the accelerating part of the wake field. From the definition of G_{\parallel} , the maximum value it can attain at the tail for $kb > 1$ is about 2.

To estimate the maximum gradient in the tail, the r dependence must also be considered. In Figure 2, the F_{\parallel} and F_{\perp} are plotted for $ka = 0.5$. Notice that the F_{\parallel} is relatively flat over the bunch cross-section, at least when $ka < 1$ which

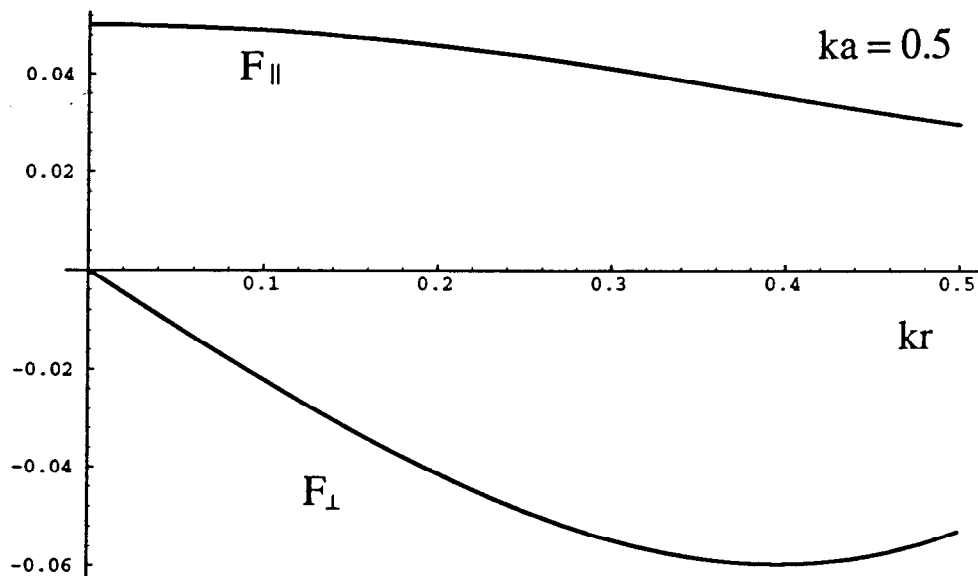


Figure 2. The radial dependence of the longitudinal and the radial wake fields for $ka = 0.5$.

seems to be a desirable regime. Note also the linearly rising F_{\perp} which gives the linear focusing of a plasma lens. To estimate realistic gradients, the F_{\parallel} is treated as flat and approximately constant, and it is replaced with its value at the origin $F_{\parallel}(0) \approx K_2(ka) + 1/2 - 2/(ka)^2$.

For the SLAC Final Focus Test Beam^[5] (FFTB) the positron bunches are completely determined except for the transverse size. The FFTB has the advantage of a very dense positron beam to excite the plasma oscillations for self-acceleration. This can always be blown up slightly from the values given in Table 1. Replacing ρ_b in (3) and gathering terms, the accelerating gradient can be put in the form

$$eW_{\parallel} = 24N \frac{r_e}{b^2} mc^2 \left[\frac{F_{\parallel} G_{\parallel}}{(ka)^2} \right] \quad (4)$$

The coefficient of the [...] term is about 3.5 MeV/cm and tuning parameters to optimize the [...] term yields a total $eW_{\parallel} \approx 5.3$ MeV/cm. The maximum occurs around $kb = 6$ and $ka = 1/1000$; the calculated plasma density is $8 \times 10^{14}/\text{cm}^3$, corresponding to Si. The relationships for a cylindrically symmetric parabolic distribution were used to relate RMS values and total lengths: $b = \sqrt{5}\sigma_z$ and $a = \sqrt{6}\sigma_x$ (assumes $\sigma_x = \sigma_y$). Compare the above gradient of 5.3 MeV/cm to the naive estimate $\sqrt{n_0}$ V/cm, or 28 MeV/cm.

At 50 GeV the positrons might traverse 5-10 cm of Si from the point of view of channeling, hence the tail could optimistically gain approximately 50 MeV. Since

Table 1. SLAC Final Focus Test Beam round beam parameters.

energy	50 GeV
coupled emittance $\gamma\epsilon$	3×10^{-5} m
β_x^*	3 cm
bunch length σ_z	0.5 mm
momentum spread $\Delta p/p$	$\pm 0.3\%$
bunch population	2×10^{10}

the bunch spread of ± 150 MeV is not coherent while the energy gain is, there is a possibility of detecting the energy increase. However, the radiative energy loss has so far been ignored.

LASER-ACOUSTIC COUPLING

Besides self-acceleration, it is natural to consider externally driven plasma oscillations as a means for accelerating particles. One such scheme is to couple a side-injected laser to an acoustic mode in the plasma.^[6] For the pure plasma case, a standing acoustic wave is set up in the plasma putting a density variation in both the ions and the plasma electrons. A polarized laser is shone on the plasma from the side, with its electric field polarized along the direction of the witness beam and the acoustic wave; see Fig. 3. The electric field of the laser drives a plasma oscillation in the electrons relative to the ions, which are nearly stationary. The time varying charge density gives rise to the electric field along the witness beam.

There are mechanical differences between acoustic waves in solids and gases. In the solid, one naively expects the acoustic wave to be carried predominantly by the ions and couple very little to the conduction electrons. If this is indeed the case, then other techniques for setting up a standing wave in the conduction electron density might have to be investigated, like using a standing wave electric field along the beam direction.

For appropriate parameters, there is an approximate resonance between the acoustic wave and the shaking of the plasma electrons. This leads to growth and then saturation of the amplitude of the plasma oscillations. The dispersion relations and condition for quasi-resonance puts restrictions on the acoustic wave and the laser. That is, the laser is chosen with a frequency just above the plasma frequency, which is the cut-off frequency for propagation of the laser in the plasma. Thus, the wavelength of the laser in the crystal is quite long. To be more definitive, let the frequency of the laser be ω_0 , and the wavevector outside the plasma be k_0 and inside be k'_0 . The 4-momentum of the acoustic wave is $(\omega_{ac} \approx 0, \mathbf{k}_r)$, and of the plasma wave is

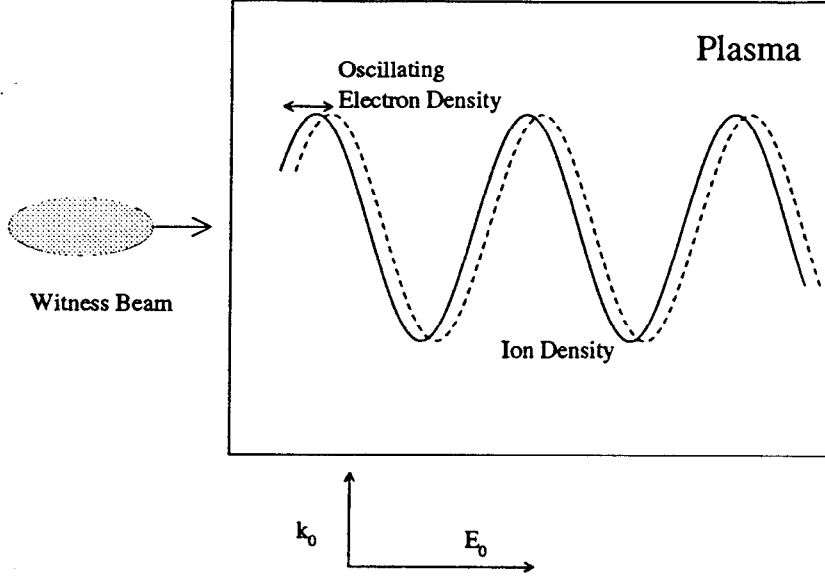


Figure 3. Side-injected laser with electric field polarized in the direction of the witness beam propagation and the acoustic wave. Figure adapted from Ref. 6.

(ω_p, k_p) . The quasi-resonance conditions are

$$\begin{aligned} \omega_0 \pm \omega_{ac} &\approx \omega_p \quad , \\ k'_0 \pm k_r &\approx k_p \quad . \end{aligned} \quad (5)$$

For quasi-resonance then (5) must be satisfied, as well as the dispersion relation for the laser inside and outside the plasma, $ck'_0 = \sqrt{\omega_0^2 - \omega_p^2}$, $\omega_0/k_0 = c$, and the dispersion relation for the acoustic wave $\omega_{ac}/k_r = v_s$, where v_s is the speed of sound in the medium. For a gas $v_s \approx 330$ m/s and for a crystal around 5000 m/s.

For a laser that is just above the cut-off frequency of the plasma, the phase velocity for the plasma oscillation is

$$v_{ph} = \frac{\omega_0 \pm \omega_{ac}}{|k_0 \pm k_r|} \approx \frac{\omega_0}{k_r} \quad . \quad (6)$$

Eqn. (6) can be parameterized as $v_{ph}/c \approx \lambda_r/\lambda_0$, where λ_r is the wavelength of the acoustic wave, and λ_0 is the wavelength of the laser in free space. From this, it is seen that the acoustic wave length must be just less than the free space wavelength of the laser.

Solving the linearized cold fluid equations for the density perturbation to the electrons, Katsouleas *et. al.* in Ref. 6 calculate the accelerating electric field to be $E_z \approx 4\pi en_1/k_r$, where the electron plasma density is $n = n_0 + \delta n \sin k_r x + n_1(x, t)$, and the velocity is $v_x = v_0 + v_1(x, t)$ where $v_0 = (-eE_0/m\omega_0) \cos \omega_0 t = -v_{os} \cos \omega_0 t$ is due to the ponderomotive force of the laser. Using these parameters, the accelerating electric field can be written

$$E_z \approx \varepsilon \sqrt{n_0} \frac{\text{V}}{\text{cm}} \quad , \quad (7)$$

$$\varepsilon = \frac{1}{4} \frac{\delta n}{n_0} \frac{v_{os}}{c} = \frac{1}{4} \frac{\delta n}{n_0} \left(\frac{eE_0}{mc^2} \right) \frac{1}{\omega_0/c} \quad .$$

The amplitude $\varepsilon = n_1/n_0$ is found from the solution of the wave equation derived from the cold fluid equations, and δn is the density fluctuation due to the acoustic wave. Ref. 6 gives several theoretical estimates on the saturation of the plasma oscillation growth due to: the wave breaking limit (an effect of the plasma thermal velocity), the detuning from the difference in the laser frequency and the plasma frequency, and the relativistic shift of the plasma frequency. Their simulations show that ε grows linearly with $\omega_p t$ and saturates with a value $\varepsilon \sim 0.10$, in their cases.

Consider for example the Brookhaven Accelerator Test Facility (ATF) RF gun^[7] and accompanying CO₂ laser. For this laser operating near the damage limit for material, 10^{13} W/cm^2 , and using the laser electric field found from $P_{laser} = E_0^2/(1200\pi)$ for SI units, the $\varepsilon \cong 0.0016$ assuming an acoustic wave with $\delta n/n \sim 0.1$. Since the laser frequency is approximately equal to the plasma frequency, the plasma density is about $10^{19}/\text{cm}^3$, corresponding to As. This gives an acceleration gradient according to Eqn. (7) of 5.0 MeV/cm. At the upgraded ATF, the electron beam can be either 50 or 10 MeV and would have an energy spread about $\pm 0.4\%$, or ± 0.2 MeV and ± 0.04 MeV respectively. To measure a net energy gain, it must be greater than the energy spread and the energy loss traversing the solid: at 5 MeV/cm this means effective acceleration over more than 0.4 mm or 80 μm , respectively.

RADIATION LOSSES

Relativistic charged particles passing through matter will radiate away some of their energy. For any acceleration scheme to be useful the particle must gain more energy than it radiates. For particles that are not trapped in between crystal planes, this is dominated by bremsstrahlung. For those particles that are confined between crystallographic planes, the radiation is synchrotron-like and is referred to as classical channeling radiation (for ultra-relativistic energies).

BREMSSTRAHLUNG

An estimate of the energy loss of a positron due to bremsstrahlung can be found in the Particle Data Book.^[8] For ultrarelativistic positrons the energy loss scale is given by the radiation length,

$$X_0 = \frac{716.4 A}{Z(Z + 1) \ln(287/\sqrt{Z})} \frac{\text{gm}}{\text{cm}^2} \quad (8)$$

For Si this is 9.4 cm; a 50 GeV positron loses about 5.3 GeV/cm initially. The solid with the least energy loss is graphite with a radiation length of 18.8 cm giving losses of 2.7 GeV/cm.

For the 50 MeV beam case considered above, it was estimated that the peak gradient from a laser-acoustic accelerator was 5 MeV/cm. For Si, the peak energy loss is about 5.3 MeV/cm, while for graphite it is about 2.7 MeV/cm. This being the case, to overcome the inherent energy spread takes twice the distance than when radiation was ignored, or the 50 MeV beam must be accelerated for a distance of about 0.85 mm not 0.4 mm.

However, at such low energies ionization effects become non-negligible. An estimate of the energy at which radiation loss from ionization and bremsstrahlung are comparable is $E_c = 800/(Z + 1.2)$ MeV. For graphite this is about 110 MeV. So, the ionization effects may even dominate the problem of energy loss.

CLASSICAL CHANNELING RADIATION OF POSITRONS

A positron that impinges on a crystallographic direction with a slight enough angle, the critical or channeling angle, will be confined between planes or between strings of atoms. Here we consider the situation when the particle is confined between planes of atoms, so-called planar channeling.^[9] The planar channeling angle, or critical angle, below which channeling can occur is given by^[10,11]

$$\psi_p = \left[\frac{2\pi Z e^2 n d_p \sqrt{3} a_{TF}}{E} \right]^{\frac{1}{2}}, \quad (9)$$

where n is the atomic density, d_p is the distance between planes, and a_{TF} is the Thomas-Fermi screening distance. See Table 2 for some estimated channeling angles.

The transverse confining potential for planar channeling defines a quantum system with the number of states^[10]

$$n_p^+ = \sqrt{0.3\gamma Z^{2/3} n d_p^3}, \quad (10)$$

for a positron of energy γmc^2 and a crystal with planar separation d_p and atomic density n . For an electron there are about 1/3 as many states as for a positron. For

Table 2. Some properties of crystals.

crystal	$n_0(\text{cm}^{-3})$	$\lambda_p = 1/k$	$\psi_p @ 50 \text{ GeV}$	$\psi_p @ 50 \text{ MeV}$
Ge	3×10^{13}	0.97 mm		
Si	8×10^{14}	0.19 mm	(110) 39 μrad	0.92 mrad
Bi	3×10^{17}	9.7 μm		
Graphite	3×10^{18}	3.1 μm		
Ni			(110) 47 μrad	1.5 mrad
Cu	8.5×10^{22}	18 nm		
Al	1.7×10^{23}	13 nm		
W			(100) 49 μrad	1.5 mrad

the Si (110) plane, with $Z = 14$, $n = 0.050 \text{ atoms}/\text{\AA}^3$, and $d_p = 1.92\text{\AA}$, the number of states is approximately $n_p^+ = 0.33\sqrt{\gamma}$. For a positron with 50 GeV in Si, $n_p^+ = 100$, and for 50 MeV there are about 3 states; for an electron with 50 GeV there are about 33 states, and for 50 MeV there is one. For channeling a positron at high energy, the classical regime is relevant, while for energies around 50 MeV it is clearly a quantum problem.

Kheifets and Knight^[12] calculate the classical channeling radiation for electrons and positrons. The radiation intensity averaged over several periods of the orbit is $I = I_0 F_b(x_m)$, where

$$I_0 = \frac{8\pi^2}{3} \gamma^2 r_e^3 mc^2 (Znd_p) \quad (11)$$

F_b is a universal function of the factor $b = 2\sqrt{3}a_{TF}/d_p$, where a_{TF} is the Thomas-Fermi screening of the atomic potential, and a function of the maximum excursion of the trajectory normalized so that $x_m = 1$ is the edge of the channel, and $x_m = 0$ is the channel center. The factors in (...) in Eqn. (11) are properties of the crystal only. Eqn. (11) is within a factor of 6 or so of what one would calculate assuming the Lenard radiation formula and a parabolic potential, instead of the much better approximation of the channeling potential due to Lindhard^[13] that Kheifets and Knight use.

In Table 3, the classical channeling radiation rate is estimated for 4 crystals. Notice the exceptionally high radiation loss rate, at least compared to the above estimate of the acceleration of around a few MeV/cm. However, the scaling with energy is such that at 50 MeV the radiation is negligible—though at this energy it is a quantum problem and is not calculated here though it is presumed small.

Table 3. Classical channeling radiation rates for a positron with 50 GeV and with a trajectory that goes to 20% of the channel width.

crystal plane	Z	n (atoms/Å ³)	d _p (Å)	a _{TF} (Å)	I(0.2)/c (MeV/cm)
Si (110)	14	0.050	1.92	0.194	210
Al (110)	13	0.060	2.02	0.199	290
Ni (110)	28	0.091	1.76	0.154	1740
W (100)	74	0.055	1.65	0.112	2600

CONCLUSIONS

From the physics mentioned above, there are several ideas, or parameters for an experiment to test acceleration in a crystal that seem possible. Again there is much more work to do on each scenario that one can imagine and on the fundamental physics that might come into to play in any given example.

For self-acceleration the beam densities required to create a high accelerating field seem restrictive. Though high energy positrons at the SLAC FFTB would probably channel effectively, their self-acceleration is difficult to observe. Also, for the driven accelerator, the gradients are too small for the energy gain to be measureable compared to the inherent energy spread. However, more work is still needed.

For lower energy beams, 50 MeV, the driven technique seems more realistic. Recall the example of driving the plasma to give a 5 MeV/cm acceleration while the bremsstrahlung losses are about 2.6 MeV/cm. Ionization can be expected to increase and perhaps double this energy loss for a non-channeled particle. Notice also that tuning the plasma does not yield a bigger gradient than 5 MeV/cm because the quasi-resonance conditions and the form for the accelerating gradient taken together do not depend on the plasma parameters. However, this currently seems the best approach for studying acceleration in solids.

REFERENCES

1. P. Chen and R. J. Noble, *Channeled Particle Acceleration by Plasma Waves in Metals*, in *Relativistic Channeling*, edited by Richard A. Carrigan and James A. Ellison, (Plenum Press, New York, 1987).
2. T. Tajima and M. Cavenago, *Crystal X-Ray Accelerator*, *Phys. Rev. Lett.* **59** (September 1987) 1440.
3. *Proceedings of the 2nd International Workshop on Laser Acceleration of Particles, Malibu, California, 1985*, edited by Chan Joshi and Thomas Katsouleas (AIP, New York, 1985).
4. Pisin Chen, *A Possible Final Focus Mechanism for Linear Colliders*, in *Particle Accelerators* **20** (1987) 171.
5. *Final Focus Test Beam Project Design Report*, SLAC-Report-376, March 1991.
6. T. Katsouleas *et al.*, *A Side-Injected-Laser Plasma Accelerator*, *IEEE Trans. Nucl. Sci.*, **NS-32**, (October 1985) 3554.
7. K. Batchelor *et al.*, *Performance of the Brookhaven RF Gun*, *Nucl. Instrum. Methods* **A318** (1992) 372.
8. *Particle Properties Data Booklet*, from *Phys. Lett.* **B239** (April 1990).
9. *Relativistic Channeling*, edited by Richard A. Carrigan and James A. Ellison, (Plenum Press, New York, 1986).
10. Donald S. Gemmell, *Channeling and Related Effects in the Motion of Charged Particles through Crystals*, *Rev. Mod. Phys.* **46** (January 1974) 129.
11. M. A. Kumakhov and F. F. Komarov, *Radiation from Charged Particles in Solids*, (AIP, New York, 1989), original in Russian, 1985.
12. S. Kheifets and T. Knight, *Full Average Radiation of Electrons and Positrons Channeled Between the Planes of a Crystal*, *J. Appl. Phys.* **50** (September 1979) 5937; S. Kheifets and T. Knight, *Radiation Spectra and Angular Distribution of Emitted Quanta for Planar Channelled Particles: Radiation of a Single Particle*, *J. Appl. Phys.* **51** (July 1980) 3863.
13. J. Lindard, K. Dan. Vidensk. Selsk Mat. Fys. Medd. **34** (1965) 18.